



Simultaneous colorimetric determination of acute myocardial infarction biomarkers by integrating self-assembled 3D gold nanovesicles into a multiple immunosorbent assay

Qinli Pu¹ · Xuanhua Yang² · Yongcan Guo³ · Tao Dai¹ · Tingyan Yang¹ · Xinying Ou¹ · Junlong Li⁴ · Shangchun Sheng⁵ · Guoming Xie¹

Received: 28 September 2018 / Accepted: 5 January 2019 / Published online: 1 February 2019

© Springer-Verlag GmbH Austria, part of Springer Nature 2019

Abstract

An improved enzyme-free immunosorbent assay is described for the simultaneous detection of the myocardial infarction biomarkers N-terminal pro B type natriuretic peptide (NT-proBNP), creatine kinase-MB (CK-MB), and cardiac muscle troponin T (cTnT). The assay integrates 3D gold nanovesicles (GNVs) and three allochroic agents (phenolphthalein, methyl red, bromothymol blue). The pH regulated allochroic agents were enwrapped in GNVs to acts as ultrasensitive nanoprobe. Loading can be controlled by adjusting the temperature to efficiently load and release the allochroic agents. This bare-eye multicolor assay has limits of detection of 70 pg·mL⁻¹ for NT-proBNP, 910 pg·mL⁻¹ for CK-MB, and 7.8 pg·mL⁻¹ for cTnT. Other features include (a) a linear range that extends over a wide range and sometimes is better than conventional HRP-based immunoassays, and (b) a precision that is comparable to immunofluorescence assays as used in the clinical laboratory.

Keywords Enzyme-free immunosorbent assay · Gold nanovesicles · Nanoprobes · Allochroic agents · Multiplex detection · N-terminal pro B type natriuretic peptide · Creatine kinase-MB · Cardiac muscle troponin T · Plasma samples

Electronic supplementary material The online version of this article (<https://doi.org/10.1007/s00604-019-3242-y>) contains supplementary material, which is available to authorized users.

✉ Guoming Xie
guomingxie@cqmu.edu.cn; xiegm059@foxmail.com

¹ Key Laboratory of Laboratory Medical Diagnostics of Education, Department of Laboratory Medicine, Chongqing Medical University, Chongqing 400016, People's Republic of China

² Department of Gastrointestinal Surgery, Second Clinical Medical Institution of North Sichuan Medical College, Nanchong Central Hospital, Nanchong, Sichuan 637000, People's Republic of China

³ Clinical Laboratory of Traditional Chinese Medicine Hospital Affiliated to Southwest Medical University, Luzhou, Sichuan 646000, People's Republic of China

⁴ University-Town Hospital of Chongqing Medical University, Chongqing 400016, People's Republic of China

⁵ Clinical Laboratory of Hospital Affiliated to Chengdu University, Sichuan 610081, People's Republic of China

Introduction

Acute myocardial infarction (AMI) is a serious life-threatening and common heart disease [1]. Creatine kinase-MB (CK-MB) is a typical biomarker of AMI. It has been reported that serum CK-MB increases with the area of myocardial infarction elevating [2]. The level of serum CK-MB can reflect the degree of myocardial damage [3]. Similarly, cardiac muscle troponin T (cTnT) is considered the best indicators and even the gold standard of myocardial damage [4]. It has great value in estimating the effect of thrombolytic therapy, predicting the area of myocardial necrosis, identifying unstable angina, etc. N-terminal pro B type natriuretic peptide (NT-proBNP) is another important AMI estimating biomarker, it can quantify the degree of severity and prognosis of AMI [5–7]. In generally, the sensitivity, specificity and timeliness of these biomarkers are different, using a single index to diagnose AMI has great limitations. Cooperative detection of CK-MB, cTnT, and NT-proBNP shows great advantages in diagnosis and prognosis of AMI [8].

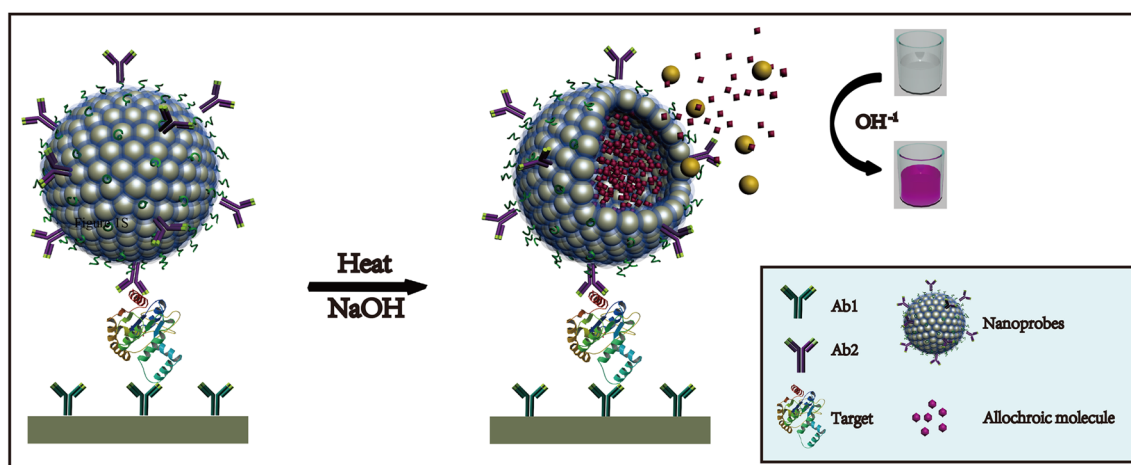
Enzyme linked immunosorbent assay (ELISA) has received widespread interests due to its superb specificity, ease of operation and bare eye signal readout [9–11]. Nevertheless, some limitations cannot be ignored in the practical application. The major drawback for conventional ELISA is the relatively low detection sensitivity and narrow linearity region compared to other technologies, such as those methods based on fluorescence [12–14] and electrochemistry [15–17]. Due to the detectable optical spectrum is generated from enzymes (horseradish peroxidase, HRP) which are conjugated to antibodies and specifically convert substrates to colored molecules [18]. The enzymatic amplification detection system is easily affected by the lab environment (pH, temperature, ionic strength, etc.), the stability of the tests is not guaranteed at some degree, the detection performance of the ELISA is largely restricted by enzymes. Besides, the multiplex detection ability of the ELISA is often astricted by the single enzyme reaction limits. Therefore, it is urgent to program and implement a new signal amplification mechanism to conquer the above mentioned limitations of conventional ELISA.

To improve the performance of conventional ELISA, efforts have been made to increase the stability and sensitivity, and to shorten the detection time [19, 20]. For example, many materials have been adopted as carriers for antibody and/or enzyme to realize signal amplification owing to the strong adsorption ability and high surface areas [21]. Some enzymatic-like materials such as Au@Pb, and MoS₂ [22, 23], can be a good alternative to HRP that used in conventional ELISA. Such improvements greatly improved the stability, detection limit and range. However, they are not applicable to the detection of multiple-level biomarkers. Therefore, many efforts have been devoted to overcoming this shortcoming by changing the original colorimetric readout to fluorescence [24, 25], electrochemical [26], and Raman spectra [27]. These methods successfully resolve the challenges in multiplex

detection, but the distinct signal output cannot be directly adapted to the conventional ELISA system, thus the advantages of ELISA have also not been good adopted. To solve the above problems, Genxi Li and coworkers have proposed improvement of immunoassay for the multiplex detection of biomarkers [28]. To avoid the effects of susceptible enzymatic reactions, the allochroic molecules triggered by acidic or basic solution as the indicators at their study. However, chromatic dyes bound to the surface of cGO through π stacking interactions are unconsolidated, the number of the combinations are also limited. In addition, it's hard to ensure the uniformity of the cGO. Therefore, the multiplex colorimetric detection of biomarkers based on the existing ELISA systems has to be further improved.

Nano-vesicles are nanoscale hollow microcapsules that have been widely explored in nanomedicine because of their unique size and intrinsic physicochemical properties [29–31]. 3D gold nanovesicles (GNVs) assembled with gold nanoparticles (AuNPs) have attracted great interests due to its excellent biocompatibility, super stability, highly homogeneity and efficient loaded and released ability. It has been extensively researched in cancer imaging and targeted drug delivery, etc. [32–34].

In this study, we report a novel enzyme-free signal amplification technique by integrating 3D GNVs loaded small allochroic dyes and immunosensor for the simultaneous detection of AMI biomarkers. The schematic of the EFISA is illustrated in Scheme 1, the principle is essentially the same as the conventional HRP-based ELISA except for the substitution of HRP with nanoprobcs. Allochroic dyes were effectively loaded in 3D GNVs, and then antibodies were conjugated on them by EDC and NSH as nanoprobcs. Heat-triggered release of allochroic molecules from captured GNVs act as indicator for quantitative determination of biomarkers. The ultrahigh sensitivity of GNVs based nanoprobcs can be easily realized by change the temperature to efficiently



Scheme 1 Schematic presentation of the principle of enzyme-free immunosorbent assay for protein detection

load and release of allochroic dyes. Conventional HRP-based ELISA often takes 20 min or more longer for final enzyme catalytic and termination reaction is essential to ensure accurate quantification. In comparison, allochroic dyes break the intrinsic limitations of enzymes. The color change triggered by acidic or basic solution can provide a simple, rapid, stable and economical signal output. Otherwise, this EFISA can simultaneously quantify different targets and has a visual readout.

Experimental

Reagents and materials

Gold(III) chloride trihydrate ($\text{HAuCl}_4 \cdot 3\text{H}_2\text{O}$, $\geq 99.9\%$), sodium citrate, N,N-Dimethyl formamide (DMF, $\geq 99\%$) and tetrahydrofuran (THF, $\geq 99\%$) were all obtained from Sigma-Aldrich Inc. (<https://www.sigmaaldrich.com/china-mainland.html>). The amphiphilic block copolymers (BCPs), PEO₄₅-b-PS₃₀₄-SH and PAA₂₃-b-PS₂₅₀-SH were purchased from Xian ruixi Biological Technology Inc. (<http://ruixibio.company.lookchem.cn/>). L-ascorbic acid (AA, $\geq 99\%$), methyl red (MR), phenolphthalein (PP) and bromothymol blue (BB), N-ethyl-N'-(3-dimethylaminopropyl) carbodiimide (EDC), N-hydroxysuccinimide (NHS), bovine serum albumin (BSA), Tween 20 and phosphate-buffered saline (PBS, 10 ×, pH 7.4) were purchased from Sangon Biotech Inc. (<https://www.sangon.com/>). Monoclonal primary antibody (Ab_1) and secondary antibody (Ab_2), standard NT-proBNP, CK-MB, and cTnT protein were purchased from Fitzgerald Industries (<https://www.fitzgerald-fii.com/>). 96-well microtiter plates (polystyrene, clear, flatbottom) were obtained from Bio-Legend Inc. (<https://www.biolegend.com/>). Deionized (DI) water (Milli-Q 18.2 M Ω -cm, Millipore System Inc. (<https://www.rephile.com/>)) was employed in all runs. All other chemicals were of reagent grade and used as received.

Instruments

The absorption spectra of the allochroic reagents were measured by a UV-vis spectrophotometer (UV-2550, Shimadzu, Japan) in the wavelength range from 300 to 800 nm. The absorption intensities in the 96-well plates were collected by a Safire2 microplate reader (Biotek ELx800, USA), and the synthesized nanocomposites were characterized with spectrophotometer (Thermo Nanodrop-1000, USA). Transmission electron microscopy (TEM, Hitachi-7500, Japan) and scanning electron microscope (SEM, SU8010, Hitachi, Japan) were employed to monitor the structures of the AuNPs and GNVs. X-Ray photoelectronic spectroscopy (XPS, Thermo ESCALAB-250, USA) was employed for elemental analysis to further investigate the successful synthesis of GNVs. The

chemical formation of AuNPs and BNP modified AuNPs were characterized by Fourier transform infrared spectrum (FT-IR, Nicolet iS50, Thermo, USA).

Allochroic agents and 3D gold nanovesicle (GNV) based enzyme-free immunosorbent assay (EFISA) for acute myocardial infarction (AMI) biomarkers

Firstly, 96-well plates were coated with Ab_1 (2 $\mu\text{g}\cdot\text{mL}^{-1}$, 100 μL per well) at 4 °C overnight. After washing the plates three times with washing buffer (10 mM PBS pH 7.4, containing 0.5% tween 20, PBST), the plates were blocked with 200 μL blocking buffer (5% BSA in PBST) for 2 h at room temperature. The plates were then washed three times with washing buffer, followed by the addition of 50 μL targets (standard NT-proBNP, CK-MB and cTnT) in dilution buffer (1% BSA in PBST). After shaking at 37 °C for 30 min, the plates were washed three times with washing buffer, and 100 μL nanoprobe ($\text{Ab}_2 @ \text{PP} @ \text{GNVs}$, $\text{Ab}_2 @ \text{MR} @ \text{GNVs}$ or $\text{Ab}_2 @ \text{BB} @ \text{GNVs}$ $\sim 0.05 \text{ mg}\cdot\text{mL}^{-1}$ in terms of Au element) was added. All the detailed steps for all material synthesis and nanoprobe construction are provided in electronic supplementary material (ESM). After 30 min reacted at room temperature, the plates were washed three times. Then 100 μL DI water was added. After being sealed with a plastic film, the plate heated to 90 °C with water bath for 20 min. Next, 50 μL NaOH solution (pH 12) was added to each well, and the plate was shaken at 600 rpm for a minute. The absorbance intensities were recorded by Safire2 microplate reader at 552 nm (PP), 434 nm (MR), 630 nm (BB).

Multiplex assay for analysis of plasma samples

Firstly, about 5 mL of human blood (The samples were collected from twenty-two pectoralgia patients and healthy individuals at university-town hospital of Chongqing medical university) was obtained in a sample tube for plasma preparation. The fresh plasma was separated from the red cells by putting the samples in an incubator at 37 °C for 30 min, and then, they were centrifuged at 1000 rpm for 10 min. For the multicolor detection of three biomarkers, 96-well plates were coated with Ab_1 mixture solution (2.5 $\mu\text{g}\cdot\text{mL}^{-1}$ of NT-proBNP, CK-MB and cTnT) at 4 °C overnight. and then all the procedures are as the same with single detection assay, except the step of addition nanoprobe (100 μL mixture nanoprobe ($\text{Ab}_2 @ \text{PP} @ \text{GNVs}$, $\text{Ab}_2 @ \text{MR} @ \text{GNVs}$ and $\text{Ab}_2 @ \text{BB} @ \text{GNVs}$ $\sim 0.05 \text{ mg}\cdot\text{mL}^{-1}$ in terms of Au element) were added for the final chromomeric reaction). The absorbance intensities were recorded by Safire2 microplate reader at 552 nm, 434 nm, and 630 nm respectively.

Results and discussion

Characterization of nanomaterials

Figure 1a illustrates the principle of preparing a functionalized nanoprobe. Firstly, monodisperse AuNPs were synthesized by sodium-citrate reduction method. Then, two BCPs were modified on the AuNPs. GNVs or allochroic dyes loaded GNVs were formed by ultrasonic. The color of the aqueous suspension (AuNPs and GNVs) presented at Fig. S2. Then, the surfaces of the GNVs were activated by coupling agents (EDC and NHS), Ab₂ were conjugated to GNVs through the EDC/NHS-mediated coupling reaction between the –COOH groups of PAA₂₃-b-PS₂₅₀-S- on GNVs and the –NH₂ groups on antibodies. The synthetic nanoprobe is abundant in capacity to capture antigens in plasma through antibody–antigen reactions. Figure 1b represents the molecular structures of two different BCPs. The BCPs modified AuNPs are characterized by fourier transform infrared spectroscopy (FTIR), and AuNPs are also measured as a comparison. The spectra of AuNPs and BCPs modified AuNPs are shown in Fig. 1c. The spectrum of BCPs modified AuNPs show some new characteristic peaks at 359 (CAromatic), 698 (Au-S), 1110 (C-O), 1493 (C=C), 756, 1452, 2923, and 3026 (C-H), compared with the spectrum of

AuNPs. The results confirm that the BCPs have been successfully linked with AuNPs through Au-S bond. Additionally, UV-vis absorption spectroscopy is employed to characterize the nanoprobe (Fig. 1d). Separate AuNPs show a characteristic adsorption peak at around 520 nm (black curve). The size changes with the particle assembling, the UV-vis absorption curve of GNVs has an obvious red shifted (red curve) compared with the AuNPs. Free Ab₂ (blue curve) have a characteristic peak at 280 nm. After conjugated on the GNVs, the Ab₂@GNVs (purple curve) present two characteristic adsorption peaks at 280 nm and 550 nm. All of the UV-vis demonstrate that the nanoprobe has been successfully constructed.

TEM is used to characterize the structure of the materials. Figure 2a, b show the TEM images of the produced AuNPs and GNVs. The nanoparticles are well-dispersed and highly uniform. The average size of the AuNPs is about 25 nm, and GNVs is about 200 nm. We also characterize the superficial and structure information of GNVs by SEM. Figure 2d shows SEM images and indicates that the GNVs have been obtained with a high purity and good uniformity. Besides, the AuNPs can be obviously seen on the surface of GNVs at high power of SEM image (Fig. 2e), which demonstrates the GNVs is self-assembled by AuNPs with the help of BCPs. After modified with Ab₂ (Fig. 2f) by coupling agents (EDC and NSH), the

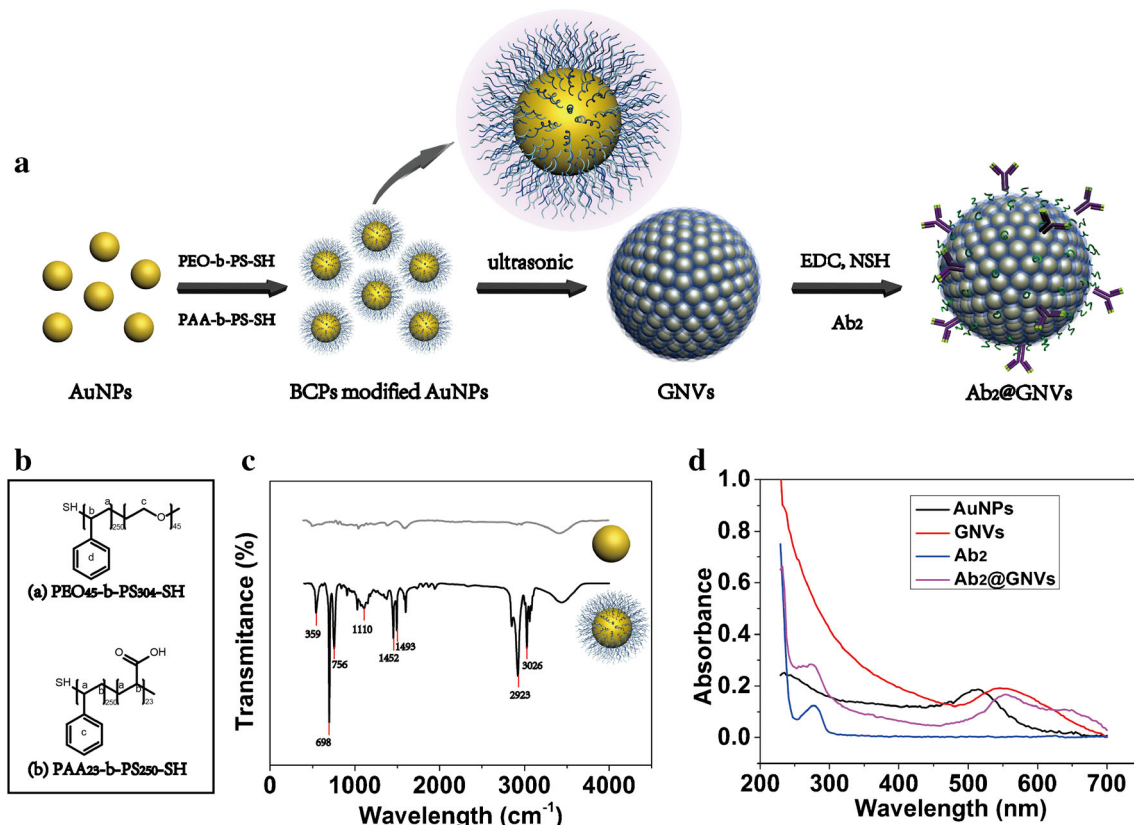


Fig. 1 a Schematic illustration of the Ab₂@GNV nanoprobe fabrication. b The chemical structure of two amphiphilic block copolymers (BCPs). c FTIR spectra of AuNPs (grey curve) and BCP-modified AuNPs (black

curve). d UV-vis spectra for AuNPs (black curve), GNVs (red curve), Ab₂ (blue curve) and Ab₂@GNVs (purple curve)

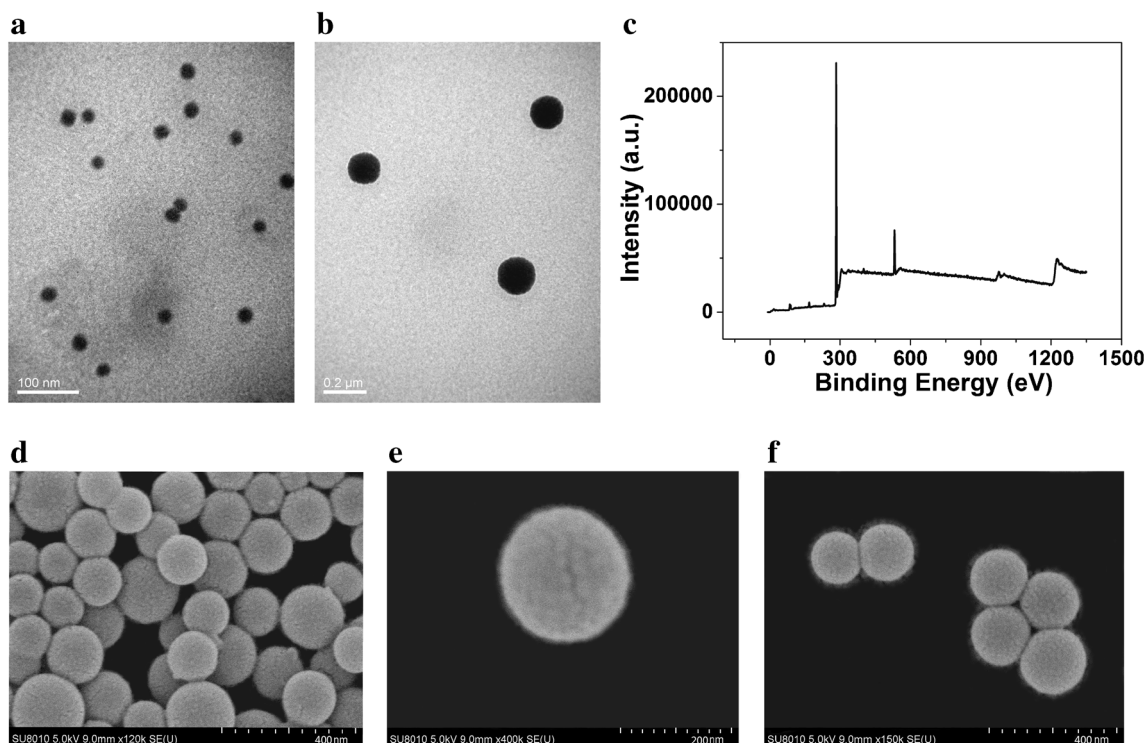


Fig. 2 **a** TEM image of AuNPs, **b** TEM image of gold nanovesicles (GNVs). **c** XPS spectra of GNVs. Low (**d**) and high (**e**) magnification SEM image of GNVs. **f** SEM image of Ab₂@GNVs

SEM image shows that the surface of the vesicles are become atomized and an increasing surface roughness compared with the GNVs. The results prove that the Ab₂ molecules are successfully modified on the GNVs. We stored the GNVs at 4 °C for three months, and the SEM image (Fig. S3) of the vesicles is also well-dispersed and unwounded, which demonstrates the synthetic GNVs have excellent stability to improve the performance of biosensors. To further verify the successful synthesis of GNVs, XPS is used to characterize the elemental composition of GNVs. As shown in Fig. 2c, the characteristic XPS peaks of Au4f7, Au4f5, O1s, S2p, N1 s and C1s are observed. Elemental analysis results fully prove the successful synthesis of GNVs.

Heat-triggered release of allochroic molecules

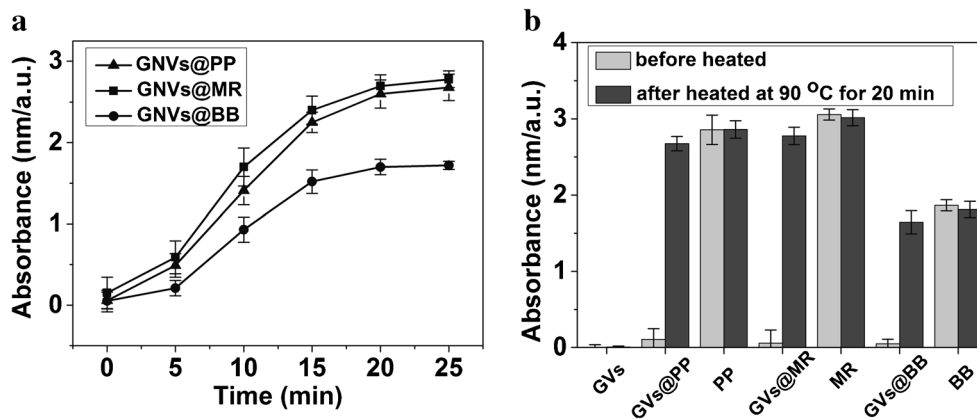
Three allochroic reagents, phenolphthalein (PP), methyl red (MR) and bromothymol blue (BB) were selected as the indicators for the quantitative analysis of targets. At the step of GNVs formation, the formed thin film (BCP-modified AuNPs) rehydrated in an aqueous suspension containing allochroic reagents. The allochroic reagents were encapsulated in GNVs by ultrasonic-mediated self-assembling. The structural representation of PP@GNVs, MR@GNVs and BB@GNVs are shown in Fig. S4A, S4B and S4C, and the colors and reversible chemical structure of three allochroic reagents are occurred under acidic and alkaline conditions.

The color vary with the change of pH are shown in Fig. S5, we can easily see the allochroic reagents present different colors at different pH conditions. Moreover, there is a good linear relationship between the UV-vis spectrum and the concentration of allochroic molecules (Fig. S6), which provides a simple, rapid, stable and economical signal output, and meet the growing biodetection requirements. Additionally, those allochroic indicators also have a good stability. Alkaline solution (NaOH, in this study) was added in allochroic aqueous suspension for coloration, and then stored for 24 h (Fig. S7) at 4 °C, the UV-vis absorbance has no significant variation. In contrast, chromogenic reaction that enzyme (such as HRP) catalyzed requires immediate detection. Therefore, the stability of the nanoprobables is more applicable to the clinical diagnosis and application.

The mechanism of nanoprobables

Due to the thermal instability of the Au – S bond at a temperature above 70 °C, the GNVs would break up, especially at 90 °C. To validate the heat-triggered release of allochroic reagents from the GNVs, the PP@GNVs, MR@GNVs and BB@GNVs (~0.5 mg·mL⁻¹ in terms of Au element) were incubated at 90 °C for a while, and then ultrasound for a minute. The released allochroic molecules have been constantly monitored every 5 min. The heat-triggered release of allochroic molecules are confirmed by UV-vis absorption spectroscopy analysis. As shown in Fig. 3a, after heated at

Fig. 3 **a** Heat-triggered release of allochroic dyes with the temperature. **b** The vary of the UV-vis absorbance spectrum (GNVs, PP@GNVs, PP, MR@GNVs, MR, BB@GNVs and BB) before and after heated at 90 °C for 20 min. Concentrations of GNVs, MR, PP and BB were kept the same for suspensions of GNVs and PP@GNVs, MR@GNVs and BB@GNVs



90 °C, the absorbance is gradually increased, indicating the successful release of allochroic molecules from GNVs. After 20 min of continuous heat-triggering, the release efficiency reaches 95%. Therefore, we chose 20 min as the hydrothermal reaction time in the following experiment. Besides, we design a series of experiments to illustrate the color signal amplification mechanism. As shown in Fig. 3b, we take equal amount of PP@GNVs, MR@GNVs and BB@GNVs ($\sim 0.05 \text{ mg} \cdot \text{mL}^{-1}$ in terms of Au element) before and after heated at 90 °C for 20 min, and then the color-reaction are triggered by NaOH. Equal concentrations of GNVs, PP, MR and BB are dealt with the same procedures as comparison. The absorbance of PP@GNVs, MR@GNVs and BB@GNVs are significantly different before and after heated. However, there is no difference at GNVs, MR, PP and BB. All the results indicate that most of the allochroic molecules have been released from GNVs, and their properties are not affected at high temperature. Furthermore, not only GNVs as the nanocarriers greatly reduce background signal of the method, but also have no disturbance for the performance of detection.

Analytical performance and selectivity of the enzyme-free immunosorbent assay (EFISA)

In the following experiments, we employ the nanoprobe as the signal amplification for the detection of AMI biomarkers, according to the principle shows in Scheme 1. As described in the introduction, the multiplexed detection of biomarkers is important for the diagnosis and prognosis of AMI. In this work, NT-proBNP, CK-MB, and cTnT are chosen as the key biomarkers of AMI. The detection is performed in commonly used 96-well plates, and the procedures for this assay are similar to conventional ELISA except for the final step of enzymatic reaction. Figure 4a, b, c display the absorbance variation for various concentrations of NT-proBNP, CK-MB, and cTnT, respectively. Here, the concentration ranges of NT-proBNP, CK-MB, and cTnT are $0.1 \text{ ng} \cdot \text{mL}^{-1} \sim 200 \text{ } \mu\text{g} \cdot \text{mL}^{-1}$, $1 \text{ ng} \cdot \text{mL}^{-1} \sim 2000 \text{ ng} \cdot \text{mL}^{-1}$ and $0.1 \text{ pg} \cdot \text{mL}^{-1} \sim 5000 \text{ pg} \cdot \text{mL}^{-1}$, respectively. The absorbance concomitantly increased with the targets concentration. Sigmoid curve regression between the absorbance and logarithms of concentrations are obtained.

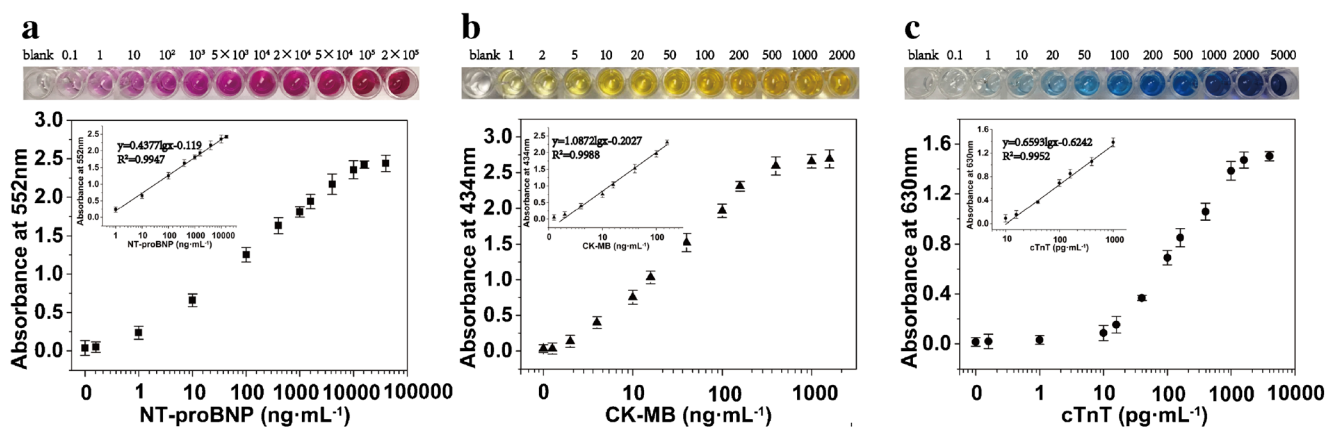


Fig. 4 **a** Representative photographs taken from the EFISA for the detection of NT-proBNP standards (from $0.1 \text{ ng} \cdot \text{mL}^{-1}$ to $200 \text{ } \mu\text{g} \cdot \text{mL}^{-1}$), and corresponding calibration plot. Inset shows the linear range region of the calibration curve. **b** Representative photographs taken from the EFISA for the detection of CK-MB standards (from $1 \text{ ng} \cdot \text{mL}^{-1}$ to $2 \text{ } \mu\text{g} \cdot \text{mL}^{-1}$), and corresponding calibration plot. Inset shows the linear

range region of the calibration curve. **c** Representative photographs taken from the EFISA for the detection of cTnT standards (from $0.1 \text{ pg} \cdot \text{mL}^{-1}$ to $5 \text{ ng} \cdot \text{mL}^{-1}$), and corresponding calibration plot. Inset shows the linear range region of the calibration curve. Error bars represented standard deviations of the measurements ($n = 3$)

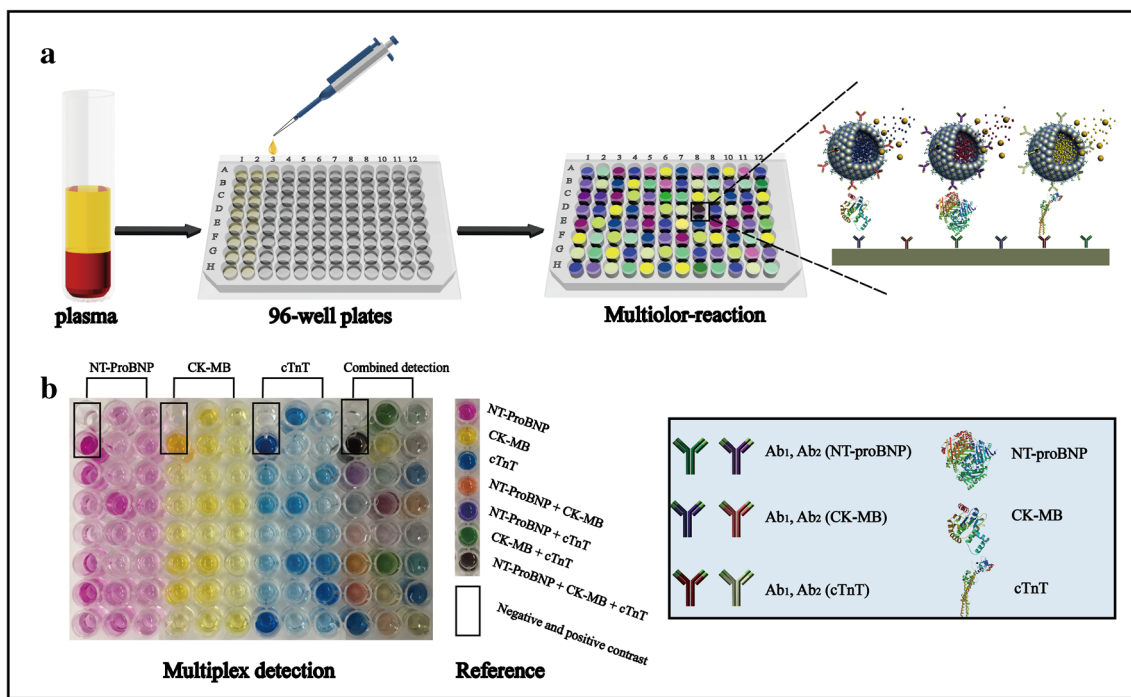


Fig. 5 **a** Schematic presentation of the principle that detects plasma samples with EFISA. **b** Representative photographs of single and multicolor detection of the collected plasma samples in PS plates. For

single biomarker detection, only one kind of relevant antibody is encapsulated in the plate. For multiplex detection, three kinds of relevant antibody are encapsulated in the plate

The linear range of detection was found to be $0.1 \text{ ng}\cdot\text{mL}^{-1} \sim 100 \text{ }\mu\text{g}\cdot\text{mL}^{-1}$ (NT-proBNP), $1 \sim 500 \text{ ng}\cdot\text{mL}^{-1}$ (CK-MB) and $10 \sim 2000 \text{ pg}\cdot\text{mL}^{-1}$ (cTnT). The limits of detection ($\text{LOD} = 3\text{SD} / k$, LOD: detection limit, SD: the standard deviation of blank sample, k: the slope of the fitting curve) are calculated to be $70 \text{ pg}\cdot\text{mL}^{-1}$ (NT-proBNP), $910 \text{ pg}\cdot\text{mL}^{-1}$ (CK-MB) and $7.8 \text{ pg}\cdot\text{mL}^{-1}$ (cTnT). Compared with conventional HRP-based immunoassays for those biomarkers (Fig. S8), the sensitivity and linearity of our assay are greatly improved. Otherwise, Reproducibility of the EFISA is further tested. Three parallel tests are used to detect different concentration of targets (Fig. S9), From the results can be conclude that the EFISA provided satisfactory reproducibility.

Multiplex detection of clinical samples

To further verify the ability of multiplex detection which is hard to realize with conventional ELISA, we coated three kinds of antibodies at 96-well plates, and three nanoprobe ($\text{PP} @ \text{Ab}_2 @ \text{GNVs}$, $\text{MR} @ \text{Ab}_2 @ \text{GNVs}$ and $\text{BB} @ \text{Ab}_2 @ \text{GNVs}$) for the simultaneous detection of NT-proBNP, CK-MB, and cTnT. We try to detect them in real serum samples (Fig. 5a). The results shows in Fig. 5b, it can be obviously seen the difference from the final colors of the liquids between the patients and healthy people. Notably, multicolor readout can be realized in a single run compared with the cumbersome one-by-one analysis of samples, and have a

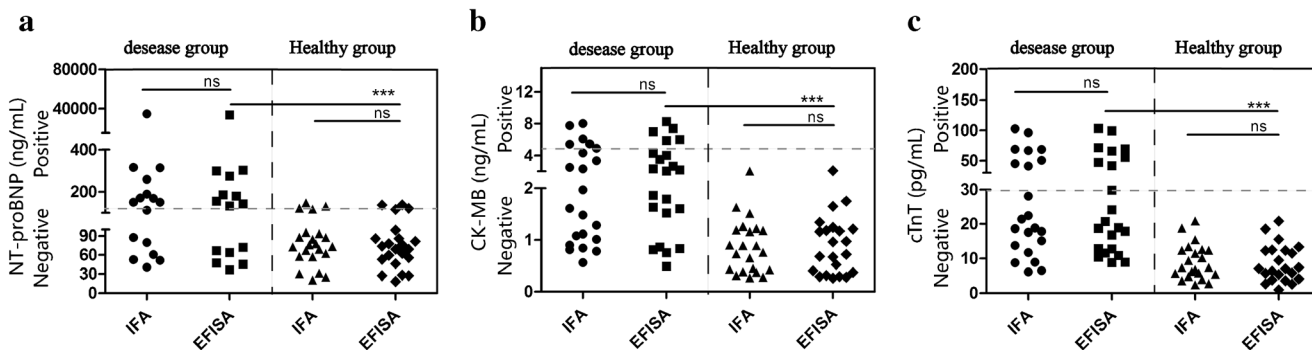


Fig. 6 Quantification of NT-proBNP (a), CK-MB (b) and cTnT (c) in the plasma of pectoralgia patients (disease group), and healthy individuals (healthy group) using EFISA, respectively. IFA and The positive signals are set to be on or above the healthy threshold (the horizontal dash line)

according to the clinical standard ($\text{NT-proBNP} > 121 \text{ pg}\cdot\text{mL}^{-1}$, $\text{CK-MB} > 4.9 \text{ ng}\cdot\text{mL}^{-1}$, $\text{cTnT} > 30 \text{ pg}\cdot\text{mL}^{-1}$). $***P < 0.001$, ns: no significant difference between the two groups

consistent results with the single analysis. In generally, the multiplex detection provides a naked-eye signal readout and more convenient method for the diagnosis and prognosis of AMI compared with the single biomarker detection. Plainly, we can easily see from the plate, not all the three biomarkers are increased at the same time in the diseased group. Therefore, omission ratio can be greatly decreased by the simultaneous detection method.

Methodological evaluation

Currently, immunofluorescence assay (IFA) is the most commonly used method for the biomarkers of AMI in clinical laboratory because of its high sensitivity and accuracy. To validate the EFISA for clinical applications, we measure the NT-proBNP, CK-MB and cTnT in human plasma samples, and the results are compared with IFA. As shown in Fig. 6a, b, c, the detailed data have been shown in the supporting information (Table S1, S2 and S3). There is no significant differences are observed between the two methods, which indicate our assay can accurately quantify the biomarkers of AMI in real samples.

Conclusions

We have combined GNVs and allochroic agents with immunosorbent assays for the simultaneous detection of AMI biomarkers. Firstly, allochroic agents break the intrinsic limitations of enzymes, the color change triggered by alkaline solution can provide a rapid, stable and economical signal output. Secondly, allochroic agents are effectively loaded in 3D GNVs, and their release is regulated by the temperature, the signal-to-noise ratio of detection is greatly increased. Moreover, our method can also realize bare eyes signal readout and multiplex detection with the three nanoprobe. Additionally, to assess the clinical applicability of the method, the simultaneous detection assay is compatible with IFA in plasma. As the universality of immunoreactions, we believe that this immunosensor reported here can also work as a versatile platform for the detection of variety low abundant biomarkers in clinical assay. In order to achieve good repeatability and better application performance of the EFISA, we have to overcome the influence of differences among nano-vesicles batches. Otherwise, nanomaterials related assays have great potential to improve the performance of the biosensors. In further studies, We wish that nanomaterials will meet challenges, and become a valuable tools for various diseases diagnosis.

Acknowledgements This research work was financially supported by the National Natural Science Foundation of China (No. 81672112, 81702101), Chongqing Technology Innovation and Application Demonstration Project (cstc2018jcsx-msybX0010) and Key Project of Education Department of Sichuan(No. 16ZA0181).

Compliance with ethical standards The author(s) declare that they have no competing interests.

Publisher's Note Springer Nature remains neutral with regard to jurisdictional claims in published maps and institutional affiliations.

References

1. Auer J, Berent R, Lassnig E, Eber B (2003) C-reactive protein and coronary artery disease. *Japan Heart J* 43(6):607–619
2. Horvath AR, Lord SJ, Stjohn A, Sandberg S, Cobbaert CM, Lorenz S, Monaghan PJ, Verhagen-Kamerbeek WDJ, Ebert C, Bossuyt PMM (2014) From biomarkers to medical tests: the changing landscape of test evaluation. *Clin Chim Acta* 427(1):49–57
3. Jaruvongvanich V, Rattanadech W, Damkerngsuntorn W, Jaruvongvanich S, Vorasettakarnkij Y (2015) CK-MB activity, any additional benefit to negative troponin in evaluating patients with suspected acute myocardial infarction in the emergency department. *J Med Assoc Thai* 98(10):935–941
4. Gerhardt W, Ljungdahl L (1998) Troponin T: a sensitive and specific diagnostic and prognostic marker of myocardial damage. *Clin Chim Acta* 272(1):47–57
5. Hunt PJ, Richards AM, Nicholls MG, Yandle TG, Doughty RN, Espiner EA (2010) Immunoreactive amino-terminal pro-brain natriuretic peptide (NT-PROBNP): a new marker of cardiac impairment. *Clin Endocrinol* 47(3):287–296
6. Shao M, Huang C, Li Z, Yang H, Feng Q (2015) Effects of glutamine and valsartan on the brain natriuretic peptide and N-terminal pro-B-type natriuretic peptide of patients with chronic heart failure. *Pak J Med Sci* 31(1):82
7. Li X, Chen C, Gan F, Wang Y, Ding L, Hua W (2014) Plasma NT pro-BNP, hs-CRP and big-ET levels at admission as prognostic markers of survival in hospitalized patients with dilated cardiomyopathy: a single-center cohort study. *J Am Coll Cardiol* 14(16):67–67
8. Fan J, Ma J, Xia N, Sun L, Li B, Liu H (2017) Clinical value of combined detection of CK-MB, MYO, cTnI and plasma NT-proBNP in diagnosis of acute myocardial infarction. *Clin Lab* 63(3):427–433
9. Liang Y, Huang X, Chen X, Zhang W, Ping G, Xiong Y (2018) Plasmonic ELISA for naked-eye detection of ochratoxin a based on the tyramine-H₂O₂ amplification system. *Sensor Actuat B-Chem* 259:162–169
10. Zhang LZ, Wang YL, Hua-Mei LU, Jian-Liang LI, Feng HU, Fu-Jin LI, Xiao YQ, Huang B, Cui YS (2018) Development of an indirect ELISA for detecting antibodies against rabbit haemorrhagic disease virus. *Chin J Prev Vet Med*
11. Pestka JJ, Azconaolivera JI, Plattner RD, Minervini F, Doko MB, Visconti A (2016) Comparative assessment of fumonisin in grain-based foods by ELISA, GC-MS, and HPLC. *J Food Prot* 57(2): 169–172(4)
12. Zhao LJ, Yu RJ, Ma W, Han HX, Tian H, Qian RC, Long YT (2017) Sensitive detection of protein biomarkers using silver nanoparticles enhanced immunofluorescence assay. *Theranostics* 7(4): 876–883
13. Sheng W, Chang Q, Shi Y, Duan W, Zhang Y, Wang S (2018) Visual and fluorometric lateral flow immunoassay combined with a dual-functional test mode for rapid determination of tetracycline antibiotics. *Microchim Acta* 185(9):404
14. Ren S, Li Y, Guo Q, Peng Y, Bai J, Ning B, Gao Z (2018) Turn-on fluorometric immunosensor for diethylstilbestrol based on the use of air-stable polydopamine-functionalized black phosphorus and upconversion nanoparticles. *Microchim Acta* 185(9):429

15. Lv H, Li Y, Zhang X, Gao Z, Zhang C, Zhang S, Dong Y (2018) Enhanced peroxidase-like properties of Au@Pt DNs/NG/cu 2+ and application of sandwich-type electrochemical immunosensor for highly sensitive detection of CEA. *Biosens Bioelectron* 112:1–7
16. Suresh L, Brahman PK, Reddy KR, JS B (2018) Development of an electrochemical immunosensor based on gold nanoparticles incorporated chitosan biopolymer nanocomposite film for the detection of prostate cancer using PSA as biomarker. *Enzyme Microb Tech* 112:43–51
17. Liu N, Yi H, Lin Y, Zheng H, Zheng X, Lin D, Dai H (2018) Combined electrochemiluminescent and electrochemical immunoassay for interleukin 6 based on the use of TiO₂ mesocrystal nanoarchitectures. *Microchim Acta* 185(5):277
18. Lequin RM (2005) Enzyme immunoassay (EIA)/enzyme-linked immunosorbent assay (ELISA). *Clin Chem* 51(12):2415–2418
19. Liu Q, Aroonyadet N, Song Y, Wang X, Cao X, Liu Y, Cong S, Wu F, Thompson ME, Zhou C (2016) Highly sensitive and quick detection of acute myocardial infarction biomarkers using In₂O₃ nanoribbon biosensors fabricated using shadow masks. *ACS Nano* 10(11):10117–10125
20. Radha Shanmugam N, Muthukumar S, Chaudhry S, Anguiano J, Prasad S (2017) Ultrasensitive nanostructure sensor arrays on flexible substrates for multiplexed and simultaneous electrochemical detection of a panel of cardiac biomarkers. *Biosens Bioelectron* 89(Pt 2):764–772
21. Li Y, Wu J, Zhang C, Chen Y, Wang Y, Xie M (2017) Manganese dioxide nanoparticle-based colorimetric immunoassay for the detection of alpha-fetoprotein. *Microchim Acta* 184(8):1–8
22. Dehghani Z, Hosseini M, Mohammadnejad J, Bakhshi B, Rezayan AH (2018) Colorimetric aptasensor for campylobacter jejuni cells by exploiting the peroxidase like activity of Au@Pd nanoparticles. *Microchim Acta* 185(10):448
23. Yigit MV, Nandu N, Hizir MS (2018) Masking the peroxidase-like activity of MoS₂ nanozyme enables label-free lipase detection. *ACS Central Sci* 4(7):862–867
24. Liang H, Jingwen YE, Jiali LI, Chen C, Guo X, Liu X, Zhong S, Jiexing LI, Laiqing LI (2018) Development and effectiveness evaluation of double label time resolved immunofluorescence assay kit for detection of CEA and NMP22 for bladder cancer. *J Mol Imaging*
25. Pan LH, Pang ST, Fang PY, Chuang CK, Yang HW (2017) Label-free biochips for accurate detection of prostate Cancer in the clinic: dual biomarkers and circulating tumor cells. *Theranostics* 7(17):4289–4300
26. Ren X, Ma H, Zhang T, Zhang Y, Yan T, Du B, Wei Q (2017) Sulfur-doped graphene-based immunological biosensing platform for multianalysis of Cancer biomarkers. *ACS Appl Mater Int* 9(43):37637–37644
27. Cheng Z, Choi N, Wang R, Lee S, Moon KC, Yoon SY, Chen L, Choo J (2017) Simultaneous detection of dual prostate specific antigens using surface-enhanced Raman scattering-based immunoassay for accurate diagnosis of prostate Cancer. *ACS Nano* 11(5):4926–4933
28. Li C, Yang Y, Wu D, Li T, Yin Y, Li G (2016) Improvement of enzyme-linked immunosorbent assay for the multicolor detection of biomarkers. *Chem Sci* 7(5):3011–3016
29. Jin HJ, Lee SH, Kim TH, Park J, Song HS, Park TH, Hong S (2012) Nanovesicle-based bioelectronic nose platform mimicking human olfactory signal transduction. *Biosens Bioelectron* 35(1):335–341
30. Liu JM, Zhang DD, Fang GZ, Wang S (2018) Erythrocyte membrane bioinspired near-infrared persistent luminescence nanocarriers for in vivo long-circulating bioimaging and drug delivery. *Biomaterials* 165:39–47
31. George J, Hayashi N, Saito T, Ozaki K, Toshikuni N, Tsuchishima M, Tsutsumi M (2017) Nanovesicle mediated delivery of combination of anticancer agents effectively induced cell death in hepatocellular carcinoma cell lines. *J Hepatol* 66(1):S462
32. Yi C, Zhang S, Webb KT, Nie Z (2017) Anisotropic self-assembly of hairy inorganic nanoparticles. *Accounts Chem Res* 50(1):12–21
33. Liu Y, He J, Yang K, Yi C, Liu Y, Nie L, Khashab NM, Chen X, Nie Z (2015) Folding up of gold nanoparticle strings into Plasmonic vesicles for enhanced photoacoustic imaging. *Angew Chem Int Edit* 54(52):15809–15812
34. Song J, Zhou J, Duan H (2012) Self-assembled plasmonic vesicles of SERS-encoded amphiphilic gold nanoparticles for cancer cell targeting and traceable intracellular drug delivery. *J Am Chem Soc* 134(32):13458–13469